CHAPTER 163

PREDICTION OF BEACH PROFILE CHANGE AT MESOSCALE UNDER RANDOM WAVES

Magnus Larson[1]

ABSTRACT: A mesoscale model is presented to calculate the average net cross-shore transport rate and beach profile evolution under random waves. Cross-shore transport formulas for random waves are derived by superimposing the transport from individual waves, which belong to an ensemble that represents the random wave field. The transport relationships for individual waves are based on experiments with monochromatic waves in large wave tanks. The model is validated using beach profile data from the SUPERTANK Laboratory Data Collection Project and three different types of profile evolution events are studied, namely equilibrium erosion with bar formation, berm flooding, and the impact of breaking waves on an offshore mound. Berm flooding includes the erosion of a well-developed summer berm and the erosion of an artificially constructed foredune, and the offshore mound tests encompass narrow- and broad-crested mounds.

INTRODUCTION

On a natural beach the random properties of the waves have a major influence on the evolution of the bottom topography. Monochromatic waves typically break in a narrow region across the profile, where incipient breaking of individual waves is a weakly random process that tends to slightly shift the location of the break point back and forth. A random wave field, however, consists of individual waves with different height, period, and direction, implying wave breaking all across the profile. The more evenly distributed forcing of random waves across shore tends to produce a profile with less pronounced morphological features as compared to monochromatic

---

[1] Coastal Engineering Laboratory, Department of Civil Engineering, University of Tokyo, 7-3-1 Hongo, Bunkyo-ku, Tokyo 113, JAPAN (Associate Professor on leave from Department of Water Resources Engineering, University of Lund, SWEDEN).

waves (Larson and Kraus 1989, 1994). Also, in a random wave field individual waves that are potentially constructive or destructive to the beach could exist simultaneously, which makes it more difficult to asses the net effect on the profile evolution (Mimura et al. 1986). Thus, when applying numerical beach profile change models to field conditions the effect of random waves on the profile development should be included through a realistic description of the hydrodynamics and net cross-shore transport rate.

Numerical models of beach profile change may be classified according to the characteristic scale employed in resolving the fluid and sediment motion. Models which attempt to describe scales of motion in time and space compatible with individual waves belong to the class of microscale models, whereas mesoscale models focus on resolving scales of motion that are the result of many waves (Larson and Kraus 1994, 1995). The numerical models by Kriebel and Dean (1985) and Larson and Kraus (1989) are examples of mesoscale models, where the local cross-shore flow pattern is not computed, and the net transport rate is derived directly from the variation in wave properties across shore. These models simulate the effect of random waves by transforming a statistical wave height measure as a monochromatic wave. Such an approach is expected to primarily reproduce the overall beach response and the details of the profile evolution will be less well predicted. For example, if the impact of a storm is simulated the total amount of material moved, including erosion on the foreshore and deposition at an offshore bar, may be in agreement with measurements, whereas the detailed shape of the bar and erosion scarp on the foreshore could differ more. Thus, treating a representative wave measure as a monochromatic wave may characterize the total forcing the profile is exposed to; however, local cross-shore variations in the forcing will be accurately described to a lesser extent.

The main objective of this paper is to present a mesoscale model to predict the net transport rate and resulting beach profile change under random waves. The randomness of the wave field is included from the start in the development of the model equations, and predictive formulas are obtained in terms of simple statistical wave properties. These properties are calculated using the random wave decay model by Larson (1995). The method of superimposing the effect of individual waves is employed for calculating the average net transport rate for a random wave field. The net transport rate distribution for individual waves is estimated from the relationships presented by Larson and Kraus (1989), which involves schematizing the beach profile into different transport regions depending on the wave characteristics. The contribution from individual waves is summed up taking into account if the wave is breaking, non-breaking, or in the swash. Profile measurements from the SUPER-TANK Laboratory Data Collection Project (Kraus et al. 1992) are used to validate the model, including such events as foreshore erosion and bar formation, berm flooding, and the transport at an offshore mound. Because the net transport rate and profile evolution are described at the mesoscale, a robust model is obtained that has potential for describing long-term profile response including seasonal changes. The

model allows the specification of long-term wave statistics as input which is needed to reproduce seasonal changes.

THEORETICAL CONSIDERATIONS

Wave Model

A successfully employed technique for modeling the decay of random waves in the surf zone is to calculate wave transformation for individual wave components in the probability density function (pdf) or spectrum, and determine the wave characteristics in the surf zone by superposition of the effect of the individual wave components (Mase and Iwagaki 1982, Dally 1992). Such a simulation technique may be computationally intensive but does not rely on any inferences about the pdf or spectrum in the surf zone (Battjes and Janssen 1978, Thornton and Guza 1983). Larson (1995) presented a model which requires the transformation of a single representative wave only; this model produces results identical or similar to a simulation that involves many wave components.

In the present profile change model, the wave transformation is described by the following equations (Larson 1995),

$$\frac{d}{dx}\left(F_{rms}\cos\theta\right) = \frac{\kappa}{d}\left(F_{rms} - F_{stab}\right) \tag{1}$$

in which,

$$F_{rms} = \frac{1}{8}\rho g H_{rms}^2 C_g \tag{2}$$

$$F_{stab} = \frac{1}{8}\rho g\left[(1-\alpha)H_n^2 + \alpha\Gamma^2 d^2\right]C_g \tag{3}$$

where H_{rms} is the root-mean-square (rms) wave height for breaking and non-breaking waves, H_n the rms wave height for non-breaking waves, α the ratio of breaking waves, C_g the group velocity, θ the incident wave angle, ρ the density, g the acceleration of gravity, d the water depth, x a cross-shore coordinate pointing offshore, and κ (=0.15) and Γ (=0.40) empirical coefficients as given by Dally et al. (1985). The wave number conservation equation and the cross-shore momentum equation are solved in parallel with Equations 1-3 to yield the wave properties and the mean water elevation across the profile.

In general, H_{rms} is obtained by employing numerical methods; this requires the specification of H_n and α at each point across shore. For a beach profile with a depth that increases monotonically with distance offshore H_n and α may be computed

directly from the local pdf, which is transformed from the offshore boundary neglecting wave breaking and truncated at the depth of incipient breaking for an individual wave. However, for a non-monotonic beach profile, such as a barred profile, an empirical closure relationship must be added to model how α is affected by wave reforming (Larson 1995). In the latter case, the non-breaking waves may consist of waves that have never been breaking (unbroken waves) and waves that were breaking but have reformed at some seaward point. A Rayleigh pdf is assumed to describe the variation in wave height in the offshore, and the sea is taken to be narrow-banded in frequency and direction.

Cross-Shore Sediment Transport Model

Relationships for the net cross-shore transport rate developed by Larson and Kraus (1989) for monochromatic waves were generalized to random waves by treating the random wave field as a collection of individual waves. Under the assumptions of linearity in transport and no interactions, the transport rate distribution generated by random waves was obtained by computing the distribution for each individual wave and then averaging over all waves according to,

$$\bar{q} = \frac{1}{N}\sum_{i=1}^{N} q_i \tag{4}$$

where $\bar{q}$ is the average net transport rate at x, N is the number of individual waves, and q_i the transport rate for wave i at x. Different transport relationships are employed depending on if a wave is breaking, non-breaking, or in the swash.

Breaking waves. If the relationship developed by Larson and Kraus (1989) for the net transport rate under breaking waves is substituted into Equation 4, the following expression is obtained for the average transport rate $\bar{q}_b$,

$$\bar{q}_b = \frac{1}{N}\sum_{i=1}^{N} K\left[D_i - (D_{eq} - \frac{\epsilon}{K}\frac{dh}{dx})\right] \tag{5}$$

where D is the wave energy dissipation per unit water volume due to wave breaking and D_{eq} its equilibrium value (Dean 1977), h the profile elevation, and K and ϵ empirical transport coefficients from the monochromatic transport relationship. In developing Equation 5 further, an assumption has to be made regarding the partitioning of the average energy dissipation between erosional and accretionary waves at all points across shore. The random wave model will predict the average energy dissipation; however, no information is obtained on the amount of dissipation that contributes to onshore and offshore transport, respectively. The simplest approach is to assume that each breaking wave at a specific water depth transports similar magnitudes of material, which leads to the following equation (Larson and Kraus 1994),

$$\overline{q_b} = K\xi\left[\overline{D} - \alpha\,(D_{eq} - \frac{\epsilon}{K}\frac{dh}{dx})\right] \qquad (6)$$

where $\overline{D}$ is the average energy dissipation per unit water volume as given by the random wave model. The function ξ automatically provides the direction of the transport and weights the influence of the erosional and accretionary waves based on the empirical criterion by Larson and Kraus (1989),

$$\xi = 2\frac{e^{-\frac{1}{M}\frac{H_{rmso}}{L_o}(\frac{wT}{H_{rmso}})^3}}{e^{-(\frac{H_{bo}}{H_{rmso}})^2}} - 1 \qquad -1 \le \xi \le 1 \qquad (7)$$

where H_{rmso} is the deepwater rms wave height, H_{bo} the wave height at incipient breaking transformed backwards to deep water, w the sediment fall speed, T the wave period, L_o the deepwater wavelength, and M (=0.00070) an empirical coefficient.

Non-breaking waves. The net transport rate seaward of the break point of an individual wave is assumed to decay exponentially with distance offshore (Larson and Kraus 1989). For a random wave field, the contribution to the transport rate from non-breaking waves is estimated to,

$$\overline{q_u} = \frac{1}{N}\sum_{i=1}^{n} q_{bi}e^{-\lambda_i(x-x_{bi})} \qquad (8)$$

where n is the number of non-breaking waves at x, x_b the breakpoint location, q_b the transport rate at incipient breaking, and λ an exponential decay coefficient, the latter two variables evaluated at x_b. Equation 8 sums the contributions to the transport rate from all waves that break landward of x. The coefficient λ depends on the median grain size and the incipient breaking wave height as for transport by monochromatic waves. Equation 8 is most easily solved by dividing the profile shoreward of x in a number of grid cells n_s and adding together the contribution from each cell to the transport rate at x. Such a method to approximate Equation 8 yields,

$$\overline{q_u} = \sum_{j=1}^{n_s} q_{bj}e^{-\lambda_j(x-x_{bj})}\Delta\alpha_j \qquad (9)$$

where $\Delta\alpha_j$ represents the increase in the ratio of breaking waves in cell j, which has a length Δx (index j denotes the grid cell number as opposed to i that denotes the number of the wave). In Equation 9, q_{bj} and λ_j must be estimated at all shoreward locations before the transport rate can be calculated.

Swash waves. The average net transport rate at a specific location x in the swash may be obtained by superimposing the transport from all waves that run up passed this location using the equation proposed by Larson and Kraus (1995),

$$\overline{q}_r = \frac{1}{N} \sum_{i=1}^{n_r} q_{si} \left(\frac{h-R_i}{h_s-R_i} \right)^{1.5} \frac{\tan\beta}{\tan\beta_s} \tag{10}$$

where q_s is the transport rate at the shoreward end of the surf zone located at x_s where the elevation is h_s and the beach slope β_s, h and β are the elevation and local beach slope at x, respectively, R is the runup height, and n_r is the number of waves that run up passed x. Equation 10 involves summing transport contributions from all waves that have runup heights exceeding the elevation where the average transport rate is calculated. Based on Equation 10, $\overline{q}_r$ is approximated in a similar manner to $\overline{q}_u$; the profile shoreward of x is divided in n_{sr} grid cells, each cell having a length of Δx, and the contribution to $\overline{q}_r$ from each cell is summed up to yield,

$$\overline{q}_r = \sum_{j=1}^{n_{sr}} q_{sj} \left(\frac{h-R_j}{h_s-R_j} \right)^{1.5} \frac{\tan\beta}{\tan\beta_s} \Delta\rho_j \tag{11}$$

where $\Delta\rho_j$ is the change along Δx in the ratio of waves that run up passed x and j denotes the grid cell number as before. The pdf for the runup height (needed to calculate $\Delta\rho_j$) may be derived using a transformation for individual wave components in the Rayleigh pdf, where each component is assumed to have a runup height which depends upon the surf similarity parameter (Battjes 1974). The corresponding distribution function $F(R)$ is obtained by integrating the pdf to yield,

$$F(R) = 1 - e^{-(\frac{R}{R_{rms}})^{\frac{2}{1-b/2}}} \tag{12}$$

where R_{rms} is defined as,

$$R_{rms} = a \, (\tan\beta_s \sqrt{L_o})^b H_{rmso}^{1-b/2} \tag{13}$$

and a ($=1.47$) and b ($=0.79$) are empirical coefficients that determine the functional dependence on the surf similarity parameter (Larson and Kraus 1989).

VALIDATION OF RANDOM PROFILE CHANGE MODEL

Profile data from the SUPERTANK Laboratory Data Collection Project (Kraus et al. 1992) were employed to examine the predictions of the model for cross-shore transport and profile change under random waves. First, the random wave model was used to calculate wave transformation in the surf zone, and then the net cross-shore transport rate distribution was determined based on the calculated wave

properties. Finally, the equation for sediment volume conservation was employed to compute depth changes.

Three different types of profile evolution tests were investigated: (1) equilibrium erosion, (2) berm flooding, and (3) waves breaking on an offshore mound. The equilibrium erosion tests involved bar development under random waves, where the profile change decreased with elapsed time as the profile approached an equilibrium configuration under the influence of a steady random wave field. Berm flooding encompassed tests where the foreshore was exposed to marked wave action, including berm and foredune erosion. Two tests were studied involving transport at an offshore mound; one mound was narrow-crested and the other mound was broad-crested. Table 1 summarizes the SUPERTANK Tests used in the model validation in terms of Test number, profile survey time, and wave conditions. The sand used in the tank had a median grain size of 0.22 mm during all SUPERTANK tests and the standard water depth employed in the tank was 3.05 m. The wave conditions in Table 1 represent target values and the generated values were slightly different (the measured wave conditions at the most seaward wave gage were used as input to the model).

Table 1.	SUPERTANK Tests used in the present study.			
Profile Event	Test No.	Time of survey	H_{rms} (m)	T_p (s)
Equilibrium erosion	ST_10	910805: 900 910806: 1100	0.57	3.0
Berm flooding	ST_90	910828: 700, 1120	0.49	3.0
	ST_A0	910828: 1500, 1637	0.49	3.0
Offshore mound	ST_J0	910908: 1100, 1610	0.49	3.0
	ST_K0	910912: 700, 1220	0.49	3.0

The preliminary calculations indicated that the initial rate of profile change was satisfactorily reproduced, whereas the development of the equilibrium profile shape was slower than expected and the shape too flat. For example, SUPERTANK Test ST_10 indicated an evolution towards a barred equilibrium profile under random waves that the model did not reproduce because of small, but significant transport rates even after long time periods. To improve the description in the model of the approach to equilibrium, Equation 6 was modified according to,

$$\overline{q_b} = K\xi\left[\overline{D} - \alpha^P(D_{eq} - \frac{\epsilon}{K}\frac{dh}{dx})\right]$$ (14)

where p is an empirical power less than one. The power p may be considered as a means of taking into account that the transport rate for an individual wave is typically

overestimated in the averaging process. Because $p < 1$, the effect on the profile development in parts of the profile where most of the waves are breaking is minor; however, if only few waves are breaking the effect of introducing p is marked. The quantity $\alpha^p > \alpha$ effectively produces a profile that is steeper than if the p is not introduced. In all calculations discussed in this paper a value of $p = 0.5$ was employed based on trial calculations with several different p-values, where comparisons were made with SUPERTANK measurements.

The values of the empirical transport coefficients in Equation 14 used in all simulations were $K = 2.0 \ 10^{-6}$ m^4/N and $\epsilon = 0.0002$ m^2/s. The value of K agrees well with the optimum value determined by Larson and Kraus (1989) for profile evolution under monochromatic waves in large wave tanks, who found an overall K-value of about $1.6 \ 10^{-6}$ m^4/N. However, ϵ determined for monochromatic waves is larger than for random waves, mainly because the profile slopes tend to grow steeper for monochromatic waves and a larger value is needed on ϵ to reduce this growth in slope. The similar coefficient values found on the K-value for monochromatic and random waves support the approach to superimpose the contribution from many individual waves to derive the transport rate distribution under random waves.

Equilibrium Erosion

In Test ST_10 random waves were employed until a near-equilibrium profile shape developed that had a distinct breakpoint bar in the offshore ($H_{rms} = 0.57$ m, $T_p = 3.0$ s). Figure 1 displays the calculated and measured profile after 400 min of wave action together with the initial profile. The calculated profile agrees quite well with the measurements, especially on the foreshore and on the seaward side of the bar. The largest discrepancies are found in the trough region, where the measurements show a more marked trough than what the model predicts. This is probably due to the oversimplification of directly relating the transport rate to the energy dissipation. The calculated average energy dissipation is a fairly smooth function across shore, which produces a smooth evolution of the bottom topography. In reality, at incipient breaking there is a pronounced local impact on the bottom, especially for plunging breakers, that could induce a marked peak in the transport rate and enhance trough development. If a large number of the waves break in approximately the same location, a marked trough could appear that the model does not reproduce.

In order to verify that the model predicted the development of an equilibrium profile for random waves, a simulation was performed using the conditions for Test ST_10 during a period of 7 days. Figure 2 displays the calculated profile at selected times, clearly showing the decrease in profile change with time elapsed. An equilibrium profile has almost developed after 3.5 days with a pronounced bar feature in the offshore.
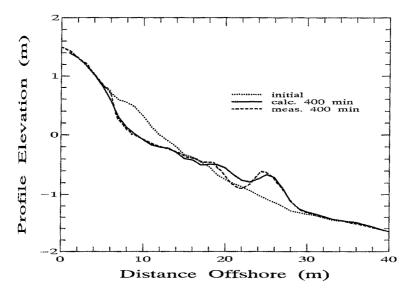
Figure 1.   Comparison between measured and calculated profile from SUPER-
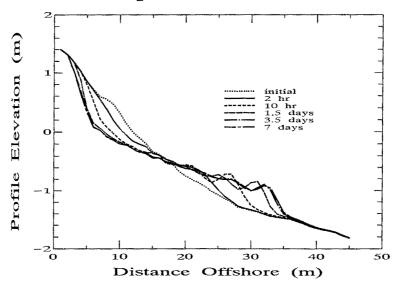   TANK Test ST_10 after 400 min of wave action.

Figure 2.   Calculated profiles at selected times for conditions as given by
             SUPERTANK Test ST_10.

Berm Flooding

SUPERTANK Tests ST_90 and ST_A0 focused on the foreshore response to random waves. In Test ST_90 the foreshore consisted of a well-developed berm that was flooded and exposed to erosive wave conditions ($H_{rms} = 0.49$ m, $T_p = 3.0$ s). Test ST_A0 involved a small foredune that was quickly eroded away by the waves (same wave conditions as Test ST_90). In both these tests the water level in the tank was 3.35 m. Figure 3 displays a comparison between calculated and measured profile for ST_90 after 50 min of wave action together with the initial profile (only the portion of the profile where any change was recorded is displayed). The model prediction somewhat underestimates the rapid response of the foreshore; in the test material was moved seaward and deposited about 10 m from the shoreward end of the tank. Also, the deposition of material occurred more evenly along the profile than what the model predicts, and the calculations tend to produce a more pronounced depositional feature. However, the overall agreement is satisfactory, which supports the transport relationship employed on the foreshore (Equation 10).
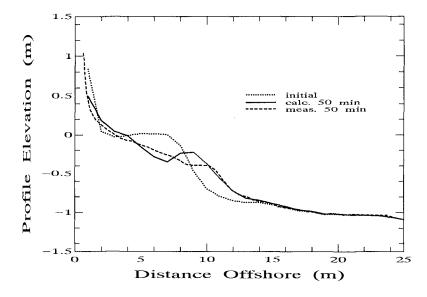

Figure 3.   Comparison between measured and calculated profile from SUPER-TANK Test ST_90 after 50 min of wave action.

In Test ST_A0 the constructed foredune eroded away very rapidly and after 10 min of wave action the foredune was completely flattened. Figure 4 shows a comparison between the model prediction and the measured profile after 10 min together with the initial profile. The calculated profile response is almost as rapid as

the measured response, and the resulting profile shape is well predicted. The transport rate formula employed in the swash zone produces onshore transport if the local slope is negative, which is the case on the shoreward side of the foredune in the beginning of Test ST_A0. Material is thus moved by the model from the foredune both in the shoreward and seaward direction, speeding up the flattening of the foredune.
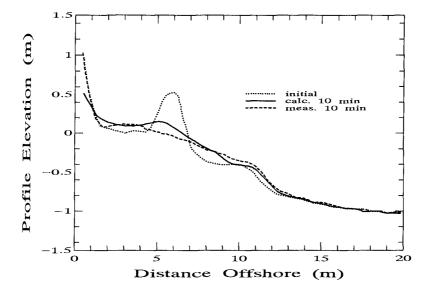

Figure 4.   Comparison between measured and calculated profile from SUPER-TANK Test ST_A0 after 10 min of wave action.

Offshore Mound

Tests ST_J0 and ST_K0 were carried out to investigate the response of an offshore mound to random waves if a large portion of the waves broke on the seaward side of the mound. For Test ST_J0 the mound was narrow-crested, whereas a broad-crested mound was constructed for ST_K0. The target wave conditions were identical to Tests ST_90 and ST_A0. A large portion of the waves broke and dissipated energy on the mound, and the effect on the foreshore of the waves that were severely broken by the mound was minor. Thus, Figure 5 shows only the profile evolution around the mound for Test ST_J0, and Figure 6 displays the corresponding region for Test ST_K0.

The narrow-crested mound deflated during wave action with some transport in the shoreward direction, although most of the material moved offshore (Figure 5). The model cannot represent such complex transport conditions and, in the model
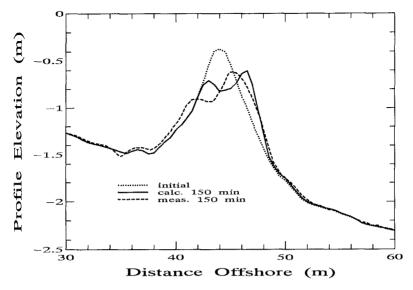
Figure 5.   Comparison between measured and calculated profile from SUPER-
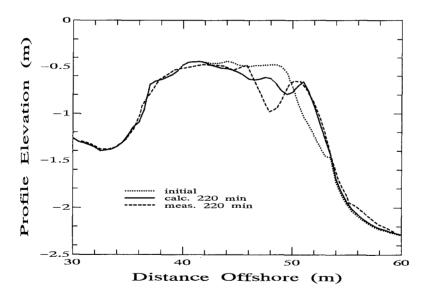   TANK Test ST_J0 after 150 min of wave action.

Figure 6.   Comparison between measured and calculated profile from SUPER-
             TANK Test ST_K0 after 220 min of wave action.

predictions, material only moved offshore. Thus, the profile development on the seaward side of the mound is reproduced by the model, whereas the model predicts no change on the shoreward side. The model was able to predict the profile response somewhat better for the broad-crested mound (Test ST_K0), because little material was pushed onshore by the waves on the shoreward side of the mound (Figure 6). The seaward shape of the mound is well predicted by the model; however, the measurements show a pronounced trough close to the seaward end of the mound that is absent in the calculations. This trough is most likely caused by the complex wave transformation occurring locally at the mound and which the random wave model is unable to represent.

CONCLUDING REMARKS

The model discussed in this paper represents one of the first attempts to consistently treat random waves in all components of a beach profile change numerical model. Previous approaches to model the profile evolution under random waves have typically involved using statistical wave measures in equations primarily developed for monochromatic waves; these models have not considered the random properties of the waves at the outset of deriving the predictive equations. The new model eliminates the problem related to selecting an equivalent monochromatic wave that reproduces a specific cross-shore phenomenon. The root-mean-square wave height is identified as the characteristic wave to be used in calculating the profile evolution under random waves with the present model.

Comparison with measured profile change under random waves from the SUPERTANK Laboratory Data Collection Project supported the technique of linearly superimposing the transport from individual waves to derive transport rate formulas for random waves. The model validation included such profile evolution events as equilibrium erosion with bar formation, berm flooding, and the impact of breaking waves on an offshore mound. In the mound tests the agreement between the model predictions and the measurements was less good compared to the other tests; this is mainly attributed to the difficulties of accurately predicting the across-shore wave properties over the mound with the random wave model. Also, the effect of the velocity asymmetry in shoaling, non-breaking waves on the mound is not described by the profile model.

After being generalized to random waves, the equation to predict the net sand transport rate in the swash zone derived by Larson and Kraus (1994) modeled profile change on the foreshore satisfactorily during erosional conditions. The model faithfully reproduced the rapid flattening of a foreshore dune indicating that the complex net transport rate distribution, where onshore transport on the shoreward side of the foredune prevailed, was well predicted. However, the model was not evaluated for accretionary conditions, and some modification might be needed regarding the local slope term to obtain a realistic description of berm build-up on the foreshore.

        The net transport rate distribution under random waves was derived without specific assumptions about the properties of the random wave field; thus, wave statistics representative for longer time periods could be used as input to the model and long-term predictions of the transport rate and profile evolution may be possible. The characteristic time scale of the profile response discussed in this paper implied that a Rayleigh pdf was a good description of the variation in wave height for the time step employed. For long-term simulations the wave statistics would have to be described by other distributions, but the calculations of the net transport rate and profile evolution could be handled within the framework of the present model. However, because the present model mainly predicts the profile response to breaking waves, additional terms that describe the transport due to non-breaking waves may have to be included to achieve a realistic profile evolution.

ACKNOWLEDGEMENTS

REFERENCES

Battjes, J.A. (1974). "Surf similarity." *Proceedings of the 14th Coastal Engineering Conference*, American Society of Civil Engineers, 466-480.

Battjes, J.A. and Janssen, J.P.F.M. (1978). "Energy loss and setup due to breaking of random waves." *Proceedings of the 16th Coastal Engineering Conference*, American Society of Civil Engineers, 569-587.

Dally, W.R. (1992). "Random breaking waves: Field verification of a wave-by-wave algorithm for engineering application." *Coastal Engineering*, 16, 369-397.

Dally, W.R., Dean, R.G., and Dalrymple, R.A. (1985). "Wave height variation across beaches of arbitrary profile." *Journal of Geophysical Research*, 90 (C6), 11917-11927.

Dean, R.G. (1977). "Equilibrium beach profiles: U.S. Atlantic and the Gulf Coasts." Department of Civil Engineering, Ocean Engineering Report No. 12, University of Delaware, Newark, DE.

Kraus, N.C., Smith, J.M., and Sollitt, C.K. (1992). "SUPERTANK Laboratory Data Collection Project." *Proceedings of the 23rd Coastal Engineering Conference*, American Society of Civil Engineers, 2191-2204.

Kriebel, D.L. and Dean, R.G. (1985). "Numerical simulation of time-dependent beach and dune erosion." *Coastal Engineering*, 9, 221-245.

Larson, M. (1995). "Model for decay of random waves in the surf zone." *Journal of Waterway, Port, Coastal and Ocean Engineering*, (in press).

Larson, M. and Kraus, N.C. (1989). "SBEACH: Numerical model for simulating storm-induced beach change, Report 1: Empirical foundation and model development." Technical Report CERC-89-9, US Army Engineer Waterways Experiment Station, Coastal Engineering Research Center, Vicksburg, MS.

Larson, M. and Kraus, N.C. (1994). "Cross-shore sand transport under random waves at SUPERTANK examined at mesoscale." *Proceedings of Coastal Dynamics '94*, American Society of Civil Engineers, 204-219.

Larson, M. and Kraus, N.C. (1995). "Prediction of cross-shore sediment transport at different spatial and temporal scales." *Marine Geology*, (in press).

Mase, H. and Iwagaki, Y. (1982). "Wave height distribution and wave grouping in surf zone." *Proceedings of the 18th Coastal Engineering Conference*, American Society of Civil Engineers, 58-76.

Mimura, N., Otsuka, Y., and Watanabe, A. (1986). "Laboratory study on two-dimensional beach transformation due to irregular waves." *Proceedings of the 20th Coastal Engineering Conference*, American Society of Civil Engineers, 1393-1406.

Thornton, E.B. and Guza, R.T. (1983). "Transformation of wave height distribution." *Journal of Geophysical Research*, 88 (C10), 5925-5938.